



## Research article

## Pilot scale manufacturing of black seed oil-loaded alginate beads; process development, and stability of thymoquinone

Hamzeh Alkhatib<sup>a,\*</sup>, Farahidah Mohamed<sup>b</sup>, Mulham Alfatama<sup>c</sup>,  
 Elham Assadpour<sup>d,e</sup>, Mohammad Saeed Kharazmi<sup>f</sup>, Seid Mahdi Jafari<sup>g,h</sup>,  
 Md Zaidul Islam Sarker<sup>i</sup>, Kishor Kumar Sadasivuni<sup>j</sup>, Awis Sukarni Mohamad  
 Sabere<sup>k,\*\*</sup>, Abd Almonem Doolaanea<sup>a,l,m,\*\*\*</sup>

<sup>a</sup> Department of Pharmaceutical Technology, Faculty of Pharmacy, University College of MAIWP International (UCMI), 68100, Kuala Lumpur, Malaysia

<sup>b</sup> Department of Pharmaceutical Technology, Kulliyah of Pharmacy, International Islamic University Malaysia, 25200, Kuantan, Pahang, Malaysia

<sup>c</sup> Faculty of Pharmacy, Universiti Sultan Zainal Abidin, Besut Campus, Kuala Terengganu, 22200, Malaysia

<sup>d</sup> Food Industry Research Co., Gorgan, Iran

<sup>e</sup> Food and Bio-Nanotech International Research Center (Fabiano), Gorgan University of Agricultural Sciences and Natural Resources, Gorgan, Iran

<sup>f</sup> Faculty of Medicine, University of California, Riverside, USA

<sup>g</sup> Department of Food Materials and Process Design Engineering, Gorgan University of Agricultural Sciences and Natural Resources, Gorgan, Iran

<sup>h</sup> Halal Research Center of IRI, Iran Food and Drug Administration, Ministry of Health and Medical Education, Tehran, Iran

<sup>i</sup> Cooperative Research, Extension & Education Services (CEES), Northern Marianas College, P.O. Box 501250, Saipan, MP, 96950, USA

<sup>j</sup> Center for Advanced Materials, Qatar University, P. O. Box 2713, Doha, Qatar

<sup>k</sup> Department of Pharmaceutical Chemistry, Kulliyah of Pharmacy, International Islamic University Malaysia, 25200, Kuantan, Pahang, Malaysia

<sup>l</sup> Sabrena Experience, 1500 Dragon Street, Suite 160, Dallas, TX, 75207, USA

<sup>m</sup> Alphastar Lab Systems, Caddo Mills, TX, USA

## ARTICLE INFO

## Keywords:

Ionic gelation  
 Alginate beads  
 Scale-up  
 Black seed oil  
 Thymoquinone  
 Stability

## ABSTRACT

The approach of ionic gelation was employed at the pilot scale of the 50 kg batch size to manufacture black seed oil (BSO)-loaded alginate (ALG) beads as a natural source supplementing the main bioactive compound of BSO, i.e., thymoquinone (TQ). The BSO-ALG emulsion was prepared by initially emulsifying BSO with alginate solution at the pilot scale in two stages. The final emulsion was then dripped through 12 units of 3D-printed multi-nozzles into a curing bath containing Ca<sup>2+</sup>. The dripping flow rate was scaled up to 288 mL/min through the 3D-printed multi-nozzles (22-gauge). The characteristics of pilot scale BSO-ALG beads were similar to those produced at the lab scale; the beads were spherical with a size of 1.84–1.94 mm. The mechanical strength and loss on drying ranged from 143.6 to 172 g and 77.85–81.96 %, respectively. The production yield and encapsulation efficiency were 77.53–83.65 % and 95.36–97.9 %, respectively. Furthermore, the emulsification process did not affect TQ stability, while the curing process reduced TQ concentration from 1.51 % to 1.03 % w/w. Additionally, a substantial drop in TQ concentration in the encapsulated BSO was observed after the drying

\* Corresponding author.

\*\* Corresponding author.

\*\*\* Corresponding author. Department of Pharmaceutical Technology, Faculty of Pharmacy, University College of MAIWP International (UCMI), 68100, Kuala Lumpur, Malaysia.

E-mail addresses: [drhamzeh@ucmi.edu.my](mailto:drhamzeh@ucmi.edu.my) (H. Alkhatib), [kishorkumars@qu.edu.qa](mailto:kishorkumars@qu.edu.qa) (K. Kumar Sadasivuni), [awissabere@iium.edu.my](mailto:awissabere@iium.edu.my) (A.S. Mohamad Sabere), [monem@iium.edu.my](mailto:monem@iium.edu.my) (A.A. Doolaanea).

<https://doi.org/10.1016/j.heliyon.2024.e37630>

Received 28 August 2023; Received in revised form 30 August 2024; Accepted 6 September 2024

Available online 10 September 2024

2405-8440/© 2024 The Authors. Published by Elsevier Ltd. This is an open access article under the CC BY-NC license (<http://creativecommons.org/licenses/by-nc/4.0/>).

process, where it reached 0.23 % w/w. Finally, the stability of BSO-ALG beads in both wet and dried forms under real-time and accelerated conditions for 3 months revealed that beads were stable in terms of their organoleptic characteristics, size and sphericity, and loss on drying. Findings from this study enable the large-scale manufacturing of encapsulated BSO and similar bioactive compounds in ALG beads for the first time. These findings are valuable for advancing microencapsulation through ionic gelation and enhancing food preservation and safety.

## 1. Introduction

Black seed oil (BSO) has been given much attention in many recent studies among herbal medicines or complementary medicines. BSO is the oil obtained via the cold-press extraction from *Nigella sativa* seeds, or what is commonly known as black cumin/black seeds [1]. The oily contents of black seeds are divided into essential (volatile) oils and fixed (stable) oils. The fixed oil constitutes about 22–38 % (w/w) and the volatile oil about 0.4–1.5 % (w/w) of the seeds [2]. The key substances for the essential oil fraction of BSO are thymoquinone (TQ), thymol, dithymoquinone,  $\alpha$ -pinene,  $\beta$ -pinene, p-cymene, and thymohydroquinone [2]. TQ is considered the main bioactive compound that adds medicinal value to BSO and constitutes about 18.4–24 % (w/w) of the essential oil and usually <2 % (w/w) of the total BSO [2,3].

Pharmacologically, TQ has anti-inflammatory and hypoglycemic effects [4,5]. It also has many other therapeutic uses, such as anti-cancer and enhancing immune responses against viral infections [6,7]. More importantly, TQ was studied and found to be a potential broad-spectrum inhibitor for the treatment of coronavirus infections [8]. It was found that TQ is not stable in oxidative, under the light, alkaline, and in the aqueous formulation conditions [9]. However, the pungent taste of BSO and the unsuitable formulation availability for children and elderly in the market indicate the importance of reformulating it suitably. The new formulation of BSO would be a natural source of TQ for these sensitive populations.

A previous study was conducted by our team to develop a new taste-masking formulation for BSO relying on encapsulation technology using sodium alginate (ALG) [10]. ALG is a hydrophilic polysaccharide sourced from brown seaweeds that is widely used for encapsulation purposes and also in biotechnical engineering [11]. This wide application is due to its practicality and excellent features of biocompatibility, non-toxicity, biodegradability, and its ability to cause water insoluble gelation in the presence of bivalent metal ions such as  $\text{Ca}^{2+}$ . ALG is known to be a whole family of linear copolymers containing blocks of (1–4)-linked  $\beta$ -D-mannuronic (M) and  $\alpha$ -L-guluronic acid (G) residues [11–13]. The ionic gelation of ALG is able to fabricate a physical barrier between a drug or supplement and the taste buds, resulting in the masking of unpleasant tastes [14]. However, scaling up the manufacturing of BSO-loaded ALG beads would facilitate making this product within reach of children and elderly, as it could be easily administered by them.

Moreover, it is essential to perform an intermediate batch scale when moving up from R&D to the production scale. This intermediate scale is called the pilot scale, which means the manufacturing of a product by following a procedure fully simulating that used for the production scale. The production on a pilot scale is enough to produce sufficient products for marketing and clinical testing [15]. Basically, scaling up the formulation of BSO-ALG beads (BABs) is achievable by understanding the concept of the ionic gelation technology to encapsulate cargoes within the matrix of ALG beads. Firstly, scaling up the emulsification process has to be done to obtain the targeted BSO-ALG emulsion. Thereafter, using a single nozzle to drip the obtained emulsion into the gelation/curing bath is usually limited to relatively small production yields where one droplet after another is produced. Mainly, increasing the production of ALG beads to reach the production scale is achievable at higher dripping flow rates of up to a hundred times, which is not applicable through one nozzle. Thus, scale-up manufacturing of ALG beads can be obtained by increasing the number of nozzles.

After the ALG beads are cured in the gelation bath, a suitable filtration and washing system for the large quantity of beads has to be used. Furthermore, another challenge in scaling up production using a multi-nozzle is that the flow rate going through each nozzle must be equal and with the same frequency of dripping. Using this approach has an important advantage in that the scale-up from lab to industrial scale is possible with low risk, for example, from one nozzle to 200 nozzles without carrying out experiments on a pilot scale (e.g., 20 nozzles) [16]. It is envisaged that in the future, encapsulating devices following the ionic gelation method will be applied at an industrial level to obtain the huge quantities required per day. However, TQ, as the bioactive compound in BSO, will be subjected to many manufacturing processes for a long time, which would affect the stability of TQ as there is a lack of studies about its stability status. This research holds significant importance as it highlights the efficacy of employing ionic gelation technology for producing BABs on a pilot scale within Good Manufacturing Practice (GMP) facilities. Furthermore, it represents a notable contribution as it is the first study, to our knowledge, to investigate both the overall stability of the manufactured BABs and the specific stability of TQ at the pilot scale. These findings are valuable for advancing food preservation and food safety.

Therefore, the current study aimed to manufacture BABs at the pilot scale of 50 kg batch size following the ionic gelation approach for the first time. This study also aimed to evaluate the effect of the pilot scale manufacturing process on the stability of TQ and to conduct both real-time and accelerated stability studies for the finished product during 3 months of storage.

## 2. Materials and methods

### 2.1. Materials

High stiffness gelation type sodium ALG IL-6G and polysorbate 80 (Tween 80) were purchased from KIMICA Co. (Tokyo, Japan) and Guangdong Runhua Chemistry Co. (Yingde, China), respectively. ALG had the following characterization: 35 % mannuronate, Mw = 97,000 Da, viscosity at 20 °C = 30–60 mPa s (1 %), Loss on Drying = 15.0 % max, heavy metals (as Pb) = 20 ppm max, pH = 6–8 (1 %), and the total bacterial count = 5000 cfu/g max. Calcium chloride dihydrate (mentioned as CaCl<sub>2</sub> in this work) was purchased from CFL-Chemische Fabrik Lehrte GmbH & Co. KG (Köthenwaldstraße, Germany). BSO was purchased from Blessed Seed Sdn. Bhd. (Kuantan, Malaysia). TQ was from Sigma-Aldrich (St. Louis, USA). Acetonitrile (HPLC grade) and methanol (HPLC grade) were purchased from Merck (Darmstadt, Germany).

### 2.2. Pre-manufacturing of the optimized BSO-ALG beads

The batch size in the current study was designed to be 50 kg of BSO-ALG emulsion (Fig. 1). Each raw material was dispensed into a polyethylene plastic bag before the pilot scale manufacturing. The scale-up to the pilot scale was performed in a controlled environment based on pharmaceutical Good Manufacturing Practice (GMP) requirements.

### 2.3. Pilot scale emulsification of BSO-ALG

All dispensed raw materials and the purified water listed in Table 1A–B were transferred into the preparation room to manufacture BABs at the pilot scale. The first step is the emulsification of BSO with the aqueous phase. Here, BSO is the oily phase, which represents 10 % w/w of the BSO-ALG emulsion and the aqueous phase represents the remaining 90 % w/w. The aqueous phase is divided into Tween 80, ALG, orange flavor, and purified water, which represent 3, 2, 1, and 84 % w/w, respectively, of the BSO-ALG emulsion formulation (Table 1A).

The emulsification process was divided into two major steps. The first step was carried out in a 100 L mixing tank to produce the initial BSO-ALG emulsion with a mechanical stirrer and a mechanical homogenizer. The second emulsification step was conducted by using a jacketed flow cell sonicator (XOLX-2000W Ultrasonic processor, Nanjing ATPIO Instruments Co., China) to produce the final homogenized nanoemulsions that would be used to formulate BABs (Fig. 1).

### 2.4. Preparation of the initial BSO-ALG emulsions

The purified water (42 kg) was transferred into the 100 L mixing tank (Fig. 1). The process parameters were set at 500 rpm and 1500 rpm for the mechanical stirrer and the mechanical homogenizer, respectively. Thereafter, the complete quantity of 1.5 kg of

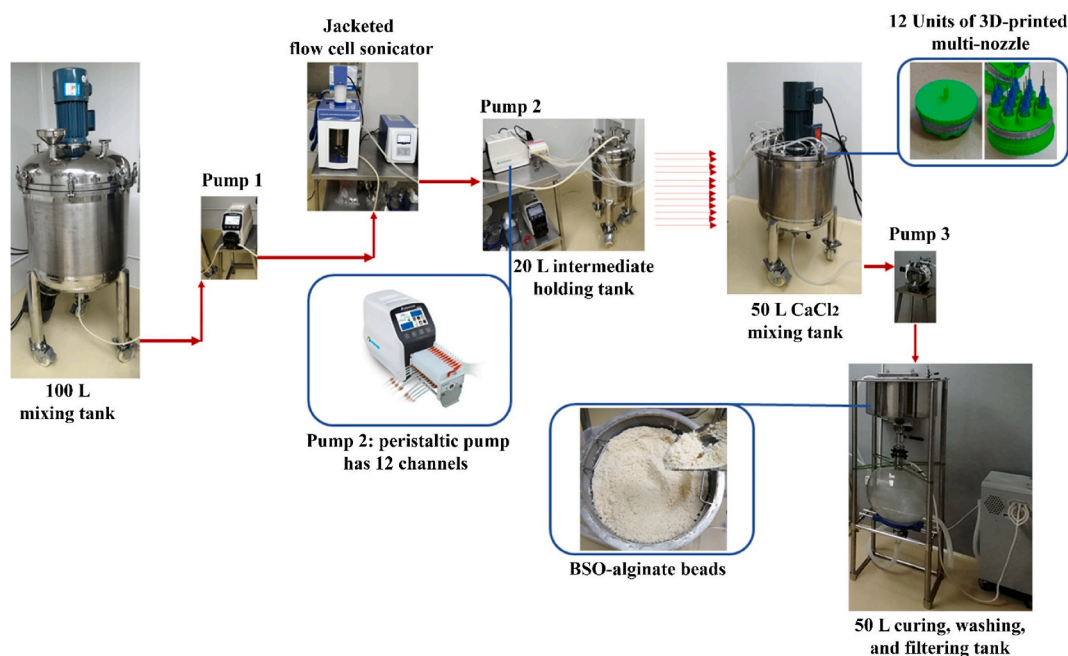


Fig. 1. Flow diagram of the pilot scale manufacturing of BSO-ALG beads.

**Table 1A**  
Ingredients of BSO- ALG emulsion and their quantity for the pilot scale dispensing.

No	Formulation ingredients	Percentage (w/w %)	Quantity per batch (50 kg)
1	BSO	10	5.00
2	ALG	2	1.00
3	Tween 80	3	1.50
4	Orange flavor	1	0.50
5	Purified water	84	42.00
Total		100	50.00

**Table 1B**  
Ingredients of the curing bath solution and their quantity for the pilot scale dispensing.

Ingredients*	Percentage (w/w %)	Quantity per lot (20 kg)
Calcium chloride	2	0.40
Purified Water	98	19.60
Total	100	20.00

\* The curing bath ingredients to prepare one lot. The dispensing was carried for 5 lots.

Tween 80 was added to the mixing tank. Tween 80 was mixed with the purified water for 5 min until it was completely dissolved. Next, the complete quantity of 1 kg of ALG was added to the obtained mixture. ALG was completely dissolved by mixing for 30 min using the same mixing parameters. Then, BSO and orange flavor of 5 kg and 0.5 kg, respectively, were completely added as the last formulation ingredients and mixed for 15 min using the same mixing parameters resulting in the initial BSO-ALG emulsion.

### 2.5. Manufacturing of the final BSO-ALG emulsions

The continuous emulsification process was followed to produce the final BSO-ALG emulsion. The initial emulsion was pumped using a peristaltic pump I from a 100 L mixing tank to a 20 L intermediate holding tank, passing through the jacketed flow cell sonicator that had the emulsification effect as shown in Fig. 1. The flow rate of BSO-ALG emulsion through the jacketed flow cell was set at 144 mL/min and the power rate of the ultrasonic processor was set at 90 %, while the chiller temperature was set at 15 °C.

### 2.6. Manufacturing of BSO-ALG beads

The manufacturing of BABs was performed by dividing the emulsion dripping process from the 20 L intermediate holding tank to a 50 L CaCl<sub>2</sub> mixing tank into 5 lots, each weighing 10 kg. The preparation of BABs for the first lot was started at 70 min from the final emulsification time. The time needed to produce 10 kg of BSO-ALG emulsion, which is the sufficient quantity to produce the beads for 1 lot, in the 20 L intermediate holding tank was ≈70 min (10 kg (9803.92 mL)/144 mL/min = 68.08 min). The density of the BSO-ALG emulsion was ≈1.02 g/mL (supplementary material).

### 2.7. Setting of the BSO-ALG beads manufacturing parameters

BABs manufacturing at the pilot scale was carried out based on the optimized parameters obtained from the lab scale studies (supplementary material). The optimized dripping flow rate of BSO-ALG emulsion through one nozzle of 22-gauge was 2 mL/min. The flow rate was upgraded to 288 mL/min and was used at the pilot scale production. The flow rate of 288 mL/min was achieved by utilizing 12 units of 3D-printed multi-nozzles, which involved 144 nozzles of 22-gauge, 12 nozzles for each unit (144 × 2 = 288 mL/min). A peristaltic pump II with 12 channels was used to pump the final emulsion from the 20 L intermediate tank into the 50 L CaCl<sub>2</sub> mixing tank (Fig. 1). Each channel was connected to one multi-nozzle and the dripping flow rate was set at 24 mL/min (24 × 12 = 288 mL/min). Moreover, the optimized concentration of 2 % w/w CaCl<sub>2</sub> as the curing bath for each lot was prepared in the 50 L CaCl<sub>2</sub> mixing tank. The purified water (19.6 kg) was transferred into the 50 L CaCl<sub>2</sub> mixing tank, and then the mechanical stirrer speed was set at 50 rpm. Thereafter, 0.4 kg of CaCl<sub>2</sub> was completely added to the purified water in this mixing tank to obtain 20 kg which complies with the optimized ratio of 2:1 w:w (curing bath:emulsion).

### 2.8. Washing and filtration of BSO-ALG beads

Once the last drops of lot 1 final BSO-ALG emulsion were dropped from the multi-nozzles into the 50 L CaCl<sub>2</sub> mixing tank, the formed beads were transferred into a 50 L curing, washing, and filtering (CWF) tank by using pump III (pneumatic pump for instant transmission), as shown in Fig. 1. The consumed curing bath solution in the 50 L CWF tank was instantly sucked from the funnel to the filter bottle connected to the circulating water vacuum pump (50 L vacuum suction filtration system, Fig. 1). The washed and filtered BABs were collected and packed in polyethylene plastic bags, which were sealed using tight cables for further studies.

## 2.9. Characterization of the manufactured BSO-ALG beads

### 2.9.1. Size and shape (sphericity)

The quantity of 10–15 manufactured BABs was randomly selected, and their photos were captured using a digital microscope (LCD Digital Microscope 4.3, Shenzhen, Guangdong, China). The length and breadth of each bead were measured using Image J software and the mean bead size was calculated. The average of the total beads was then calculated [10]. The sphericity of the bead was determined by calculating the sphericity factor (SF) based on equation (1). Beads with SF < 0.05 were considered spherical [17].

$$SF = \frac{(D_{max} - D_{min})}{(D_{max} + D_{min})} \quad (1)$$

Relative Standard Deviation (% RSD) was calculated to determine the uniformity of the produced beads by equation (2) [18]:

$$\% RSD = \frac{\text{Standard deviation of beads size}}{\text{Size mean of the measured beads}} \times 100 \quad (2)$$

### 2.9.2. Mechanical strength

Five BABs were selected randomly from each lot. The mechanical strength of each single bead was measured by a CT3 Texture Analyzer (Brookfield Laboratories, Middleboro, USA) following the method of Erdem et al. [19]. Each bead was compressed by a cylinder probe (25 mm diameter) with a deformation setting of 1 mm. The test speed and trigger load were set at 1 mm/s and 2 g, respectively. The average of five measurements was then calculated [20].

### 2.9.3. Loss on drying (LOD)

LOD of BABs was determined for each manufacturing lot through the method reported by Maharjan et al. [21]. The beads (1 g) were placed in a Petri dish and then dried overnight at 60 °C in an oven. LOD was calculated by equation (3):

$$LOD (\%) = 100 - \left( \frac{(W_4 - W_3)}{(W_2 - W_1)} \times 100 \right) \quad (3)$$

where W1 is the weight of an empty Petri dish before drying, W2 is the weight of a Petri dish with beads before drying, W3 is the weight of an empty Petri dish after drying, and W4 is the weight of a Petri dish with beads after drying.

### 2.9.4. Production yield

The total quantity of BABs for each pilot scale manufacturing lot was weighed, and then the production yield was calculated by equation (4):

$$\% \text{ Yield} = \frac{\text{Weight of the beads after curing}}{\text{Weight of the pumped material into curing bath}} \times 100 \quad (4)$$

### 2.9.5. Encapsulation efficiency (EE)

Quantification of BSO in the produced BABs was determined by following an emulsification-spectroscopic method developed and validated by our team [22]. The manufactured BABs (1 g) were dispersed in a phosphate buffer solution at pH = 6.8 to a total weight of 50 g. The beads were shaken in the phosphate buffer until they were completely dissolved. The newly produced emulsion (10 mL) after dissolving the ALG beads was taken and sonicated at 10 % power rate for 120 s, then analyzed by UV-Vis spectrophotometer (UV-1800 240V, Shimadzu, Tokyo, Japan) at the optimal wavelength of 400 nm to obtain the absorbance and the concentration of BSO in the ALG beads. EE was calculated as a percentage of the actual amount of BSO in the ALG beads to the theoretical amount.

## 2.10. The effect of pilot scale manufacturing process on the stability of TQ

The manufacturing processes to produce BABs in this study were divided into the initial emulsification process, the final emulsification process, BABs fabrication, and BABs drying in the case of dried beads as the finished product. The quantification of TQ in all samples was analyzed by HPLC using the validated stability-indicating method used in our previous study [10]. The analysis was performed on the Shimadzu LC-20AT HPLC system (Japan). A mixture of acetonitrile and water in the ratio of 60:40 v:v was used as the mobile phase at a flow rate of 1 mL/min on an Inspire C18 (4.6 × 250 mm, 5 μm) analytical column. The detection was performed at a wavelength of 254 nm using a diode-array detector. Here, the injection volume and run time were 20 μL and 10 min, respectively.

### 2.11. Stability study

The stability study was performed on both wet and dried BABs. The beads were packed in 50 mL glass bottles. The bottles were stored in stability chambers under real-time (30 °C, 75 % RH) and accelerated (40 °C, 75 % RH) conditions [23,24]. The samples were collected at the designed stability points of 0, 1, 2, and 3 months. The organoleptic characteristics were investigated using a visual examination method [25]. The physical appearance, color, oil leakage, and water squeezing were studied for both real-time and accelerated conditions.

## 2.12. Statistical analysis

The statistical analysis in the current study was carried out using Minitab software, version 17.1.0. The data obtained from the characterization of the pilot scale manufactured beads and stability study were analyzed using One-Way ANOVA followed by a Tukey Post-Hoc test. All characterization and stability data were analyzed in triplicate ( $n = 3$ ) except for the data of beads measurement and mechanical strength, where  $n = 10$ – $15$ , and  $n = 5$ , respectively.

## 3. Results and discussion

### 3.1. Washing and filtration of BSO-ALG beads

$\text{CaCl}_2$ , among calcium salts, has a notable bitter taste and exhibits a salty taste at medium and high concentrations [26]. Since BABs formulation was designed for taste-masking purposes, it is recommended to have no other source of salty taste or bitterness. This leads to the necessity of removing the residues of  $\text{CaCl}_2$  on the surface of the produced beads, which would improve the taste on the one hand and stop the action of calcium ions on ALG chains on the other. However, there were not many details in previous studies about washing the ALG beads after the fabrication process for encapsulation purposes, as those studies were performed at the lab scale and the beads were simply washed with distilled water [27,28]. In fact, washing and filtration of ALG beads at a lab scale are easily applicable as the number of beads is small, which needs simple equipment such as beakers and distilled water for washing and simple mesh for filtration. Washing and filtration as a final step to manufacture BABs at the pilot scale is a critical step to avoid the unacceptable  $\text{CaCl}_2$  taste and to inhibit the chemical interactions between  $\text{CaCl}_2$  residues and ALG chains. Also, the washing and filtration step at the pilot scale is more complicated as the process has to be carried out in large quantities in a short time.

Utilizing the 50 L vacuum suction filtration system (Fig. 1) made the process much easier because of the presence of the circulating water vacuum pump that was able to apply an instant suction for the curing bath solution or the washing water from the funnel to the filter bottle. As shown in Fig. 2, the concentration of calcium ions in the washing water reduced significantly from 0.434 mg/mL in the first round to 0.087 mg/mL in the second washing round ( $p < 0.05$ ). This reduction indicates that  $\text{CaCl}_2$  residues were being removed from the surface of BABs as more washing rounds were applied, where a significant reduction in calcium ion concentration was indicated at the third washing round ( $p < 0.05$ ). The concentration of calcium ions was stabilized at the third washing round and so on, as there were no significant differences in calcium ion concentrations in the washing water after the third round ( $p > 0.05$ ). The concentrations ranged between 0.012 and 0.0002 mg/mL (Fig. 2). In light of these results, the number of rounds required to wash one manufacturing lot of BABs was three, using 20 L purified water for each round. Applying three washing rounds would be carried out in a short time while waiting for the next lot to be dripped down into the 50 L  $\text{CaCl}_2$  mixing tank.

### 3.2. Characterization of the pilot scale manufactured BSO-ALG beads

#### 3.2.1. Size and sphericity

The particle size has the ability to influence the encapsulated material distribution, release rate, degradation rate, and the administration route of the formulation. This shows the importance of the ALG bead size as a parameter for the evaluation of particles' properties during the droplet fabrication step and the manufacturing process [29]. The size of the pilot scale manufactured BABs was individually measured for each lot as well as their sphericity. The size of BABs was found to be homogeneously manufactured among all 5 lots with no significant differences ( $p > 0.05$ ), as shown in Fig. 3. The size of the beads ranged between 1.84 and 1.94 mm (Fig. 3a and b). Although the %RSD values were detected to be higher at the pilot scale compared with the lab scale (supplementary material), the Standard Deviation (SD) values were confined between 0.09 and 0.17 mm (Fig. 3a and b), indicating the narrow size distribution, which is still within the acceptable range of ALG beads size to be used as a solid oral formulation designed for children. Lopez et al. [30] reported that solid medications with a size  $< 2.5$  mm are suitable to be easily administered by paediatric. Moreover, the concentration

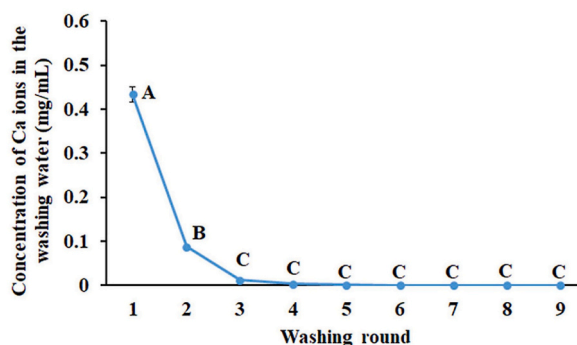


Fig. 2. Concentration of  $\text{Ca}^{2+}$  at each washing round. Different letters indicate significant differences among means ( $p < 0.05$ ). Error bars represent the standard deviation of the mean values ( $n = 3$ ).

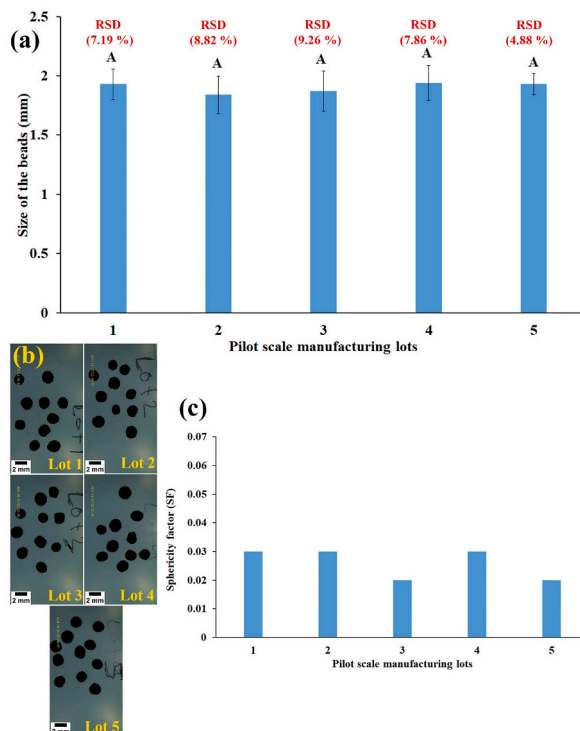


Fig. 3. Size (a), captured images (b), and sphericity (c) of BSO-ALG beads at each manufactured lot. Different letters indicate significant differences among means ( $p < 0.05$ ). Error bars represent the standard deviation of the mean values ( $n = 10-15$ ).

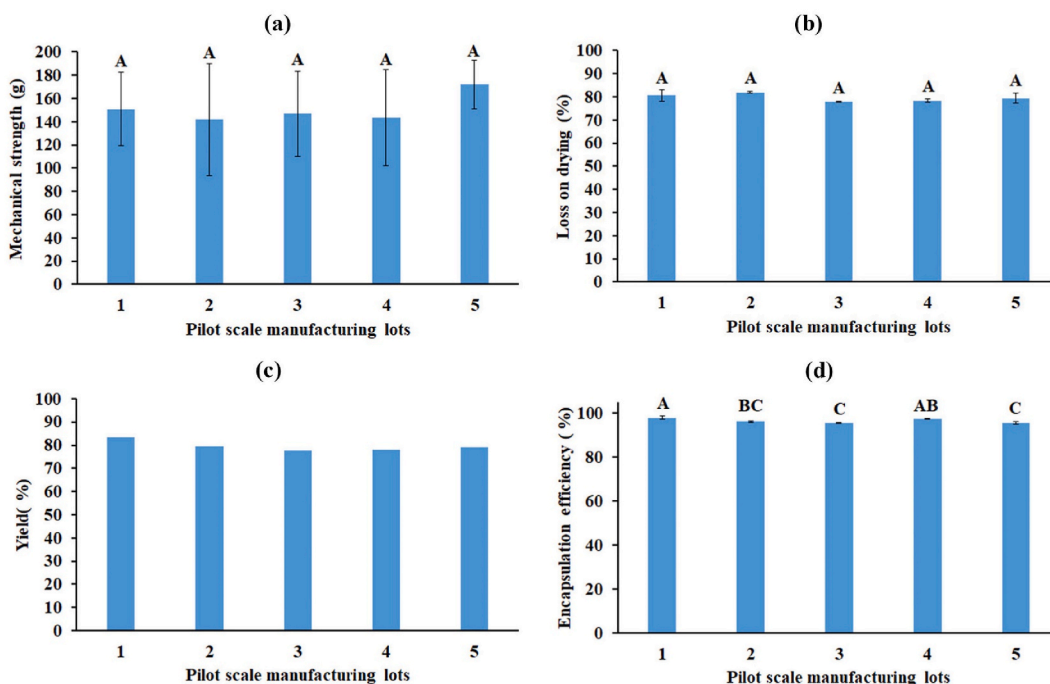


Fig. 4. Mechanical strength (a), loss on drying (b), yield (c), and encapsulation efficiency (d) of BSO in BSO-ALG beads at each manufactured lot. Different letters indicate significant differences among means ( $p < 0.05$ ). Error bars represent the standard deviation of the mean values ( $n = 5$  for the mechanical strength data and  $n = 3$  for the loss on drying and encapsulation efficiency data).

of ALG in the formulation, nozzle diameter, dripping distance, curing bath, and dripping flow rate are factors that could affect the size and shape of ALG microspheres, as mentioned by Uyen et al. [31] and Agüero et al. [29]. These parameters were all optimized at the lab scale, as all-variable ranges were selected to be suitably used at the pilot scale (supplementary material).

The large quantity of dripped BABs in the 50 L CaCl<sub>2</sub> mixing tank reduced the dripping distance and concentration of the curing bath as the volume was increasing continually during the BSO-ALG emulsion dripping process. The total number of nozzles involved in the current study was 144, distributed in 12 units of multi-nozzle, each with 12 nozzles. The dripping flow rate had to be 2 mL/min per nozzle as it was optimized on the lab scale; the higher flow rate of 3 mL/min produced irregular beads. Additionally, the defect in any individual nozzle could increase the flow rate at other nozzles in the same unit of multi-nozzle that would produce beads or particles with irregular shapes or with sizes >2.5 mm. These challenges at the pilot scale could be the reason behind the higher % RSD values. However, the manufactured BABs at the pilot scale were considered spherical on average, as the SF values were <0.05 among the all-manufacturing lots (Fig. 3c). Uyen et al. [31] mentioned that ALG concentration in the formulation is a major factor that affects the shape of ALG beads, where irregular shapes were obtained when ALG concentration was low (based on preliminary experiments), which is in agreement with the current study. The all-optimized parameters were working as one system that was challenging the large-scale difficulties to produce the spherical BABs within an acceptable size.

### 3.2.2. Mechanical strength and loss on drying

The mechanical strength of ALG/hydrogel beads is one of the most important physical properties that is significantly associated with other properties such as storage stability, texture feeling in the mouth cavity, and controlled release [32]. The suitable mechanical strength also indicates stability during processing and works to protect the hydrogel beads against bursting or smashing during transportation processing [33]. The mechanical strength of BABs ranged between 143.6 and 172 g, with no observation of any significant differences among all 5 pilot scale manufacturing lots ( $p > 0.05$ ), as shown in Fig. 4a. The mechanical strength results were also clearly harmonized with the LOD of the manufactured BABs (Fig. 4b). There were no significant differences between LOD in all manufacturing lots ( $p > 0.05$ ). LOD in the manufactured BABs was confined between 77.85 and 81.965 %, as shown in Fig. 4b.

The mechanical strength and LOD of BABs fabricated at the lab scale ranged from  $158.7 \pm 22.24$  g to  $162.4 \pm 33.9$  g and  $79.06 \pm 0.68$  % to  $79.89 \pm 0.09$  % (supplementary material), which are in agreement with the obtained results at the pilot scale. This agreement is considered a verification of the efficacy of optimized parameters to provide enough curing to the beads at the pilot scale. It has been reported by Cao et al. [34] that many factors could affect the mechanical strength of ALG beads, such as ALG molecular weight, ALG concentration, the percentage of guluronic acid (internal factors), and the concentration of calcium ions (external factor). The impact of internal factors was not studied in the current study as the ALG polymer was selected and its concentration was optimized at 2 % w/w based on other variables, namely the bead size, bead sphericity, and EE. For the curing bath concentration as an external factor, it was a critical variable up to 1 % w/v, then the impact was stepped down with no significant changes in the beads' mechanical strength and LOD in the curing bath range of 1–2 % w/v for CaCl<sub>2</sub> solution (supplementary material). So, the curing bath concentration was set at 2 % w/w at the pilot scale manufacturing level, which was effective in producing BABs with similar mechanical strengths and LOD properties as they were designed on the lab scale.

### 3.2.3. Production yield and encapsulation efficiency

Determination of the production yield at the pilot scale plays an important role in designing other manufacturing steps, such as the primary packaging, where the number of packaging containers for the complete manufacturing batch is decided based on the quantity of BABs produced. However, the production yield of BABs at the lab scale optimization studies was  $78.17 \pm 1.34$  %, which is in agreement with the crosslinking behavior that squeezed out some of the aqueous phases, resulting in low yield (supplementary material). A similar reduction in the manufacturing yield of BABs at the pilot scale was observed to be between 77.53 % and 83.65 %, with an average of  $79.64 \pm 2.39$  % (for 5 lots), as shown in Fig. 4c.

The characterization studies of the beads produced at both the lab and pilot scale indicate the harmony of the gelation process at the optimized parameters to encapsulate BSO in the ALG beads. Firstly, the crosslinking process squeezed out some of the aqueous phases that gave the beads specific mechanical strength, which then resulted in a lower production yield associated with water loss. Moreover, the high EE of BSO in the ALG beads among all the manufacturing lots (Fig. 4d) confirms that the main factor behind the reduction of production yield is the lost water during the gelation process. Statistically, some significant differences in the EE were detected among the manufacturing lots ( $p < 0.05$ ), as shown in Fig. 4d. However, the lowest and highest EE were detected at  $95.36 \pm 0.55$  % and  $97.9 \pm 0.64$  %, respectively. Additionally, there was no significant difference between the EE at the manufacturing lots 1 and 4 ( $p > 0.05$ ) and between the manufacturing lot 2, 3, and 5 ( $p > 0.05$ ). There was also no significant change in the EE between the manufacturing lot 2 and 4 ( $p > 0.05$ ), as shown in Fig. 4d.

The encapsulation of edible oils within ALG beads following the external gelation mechanism has been previously reported to have high EE. It could be due to the type of ALG with a high G content (guluronic acid) and the stability of emulsions before the dripping process [35]. An EE = 98.30 % of linseed oil in ALG beads was reported by Piornos et al. [35], where the encapsulation process was associated with the lupin protein as an emulsifier. In another study, the *Sacha inchi* oil was encapsulated in ALG beads with the aid of a non-ionic surfactant (Tween 20) that obtained an EE > 99 % [36]. The stability of the emulsions prevented the leakage of BSO out of the beads during the gelation process in the curing bath, which led to the high EE. It is a challenge at the pilot scale to emulsify the quantity of 50 kg. EE obtained at the pilot scale indicates the high efficacy of the emulsification process to produce the optimized emulsion that would be dripped for the gelation process. However, the variation in the obtained results of 2.54 % between the lowest and highest values of EE at the pilot scale may be attributed to the relatively long duration of the emulsification process. This long time would affect the homogenous distribution of BSO among the emulsions in the 20 L holding tank before the dripping process.



### 3.3. The effect of the pilot scale manufacturing process on the stability of TQ

Both the initial and final emulsification processes did not have any statistically significant effect on the stability of TQ in the emulsified BSO ( $p > 0.05$ ), as shown in Fig. 5. Firstly, the concentration of TQ in the raw BSO was found at  $1.51 \pm 0.009$  % w/w. Thereafter, it was found in the initial and final BSO-ALG emulsions at  $1.33 \pm 0.13$  % w/w and  $1.44 \pm 0.02$  % w/w, respectively. However, the reason behind the small variation in the TQ concentration in the emulsified BSO might be attributed to the homogenous distribution of the BSO in the continuous phase, as the result was found to have a lower SD at the final emulsion that was produced using the ultrasonication process.

Moreover, the retention of TQ in the encapsulated BSO in ALG beads was significantly affected ( $p < 0.05$ ), as the concentration of TQ in the BSO after the gelation process in the curing bath was  $1.03 \pm 0.17$  % w/w (31.7 % difference compared with the raw BSO). Although the gelation process significantly reduced the concentration of TQ in the encapsulated BSO, the total concentration in the fabricated BABs was found at  $1.31 \pm 0.22$  mg/g, which is close to the TQ concentration obtained in the BSO-ALG emulsion (Fig. 5). It means that the quantity of BSO in 1 g beads was  $>$  the quantity of BSO in the emulsions due to the aqueous phase loss from the fabricated beads during the gelation process. In other words, about 1.25 g of BSO-ALG emulsion was used to fabricate 1 g of BABs (% Y  $\approx 80$ ). This aqueous phase loss during the gelation process could contain some TQ that could be dissolved in the aqueous phase due to the presence of Tween 80. It has been reported by Rahat et al. [37] that surfactants enhance the solubility of TQ.

In addition to the emulsification and gelation processes, the effect of the drying process on the stability of TQ was evaluated. TQ content in the dried BABs was 1.47 mg/g, indicating a remarkable loss in TQ concentration in BSO as the BSO quantity in 1 g of the dried beads is 5 folds of the quantity in 1 g of the wet beads (LOD  $\approx 80$  %). However, the concentration of TQ in the encapsulated BSO in the dried beads was significantly dropped ( $p < 0.05$ ) to 0.23 % w/w (84.7 % difference compared with the raw BSO), as shown in Fig. 5. TQ is particularly part of the essential oils (volatile) of the BSO [2]. The volatile compounds tend to evaporate easier than water [38], and as explained earlier, Tween 80 could assist in dissolving some of the TQ in the aqueous phase, which would lead to TQ loss during water evaporation in the drying process. In a study by Baldim et al. [38], about 75–90 % retention of thymol, as the bioactive compound in the *Lippia sidoides* essential oil, was achieved after the fabrication process of spray-dried lipid nanoparticles. The variation in the thymol retention was due to the solid material content in the formulation; higher thymol retention was indicated at the higher solids content.

In another study by Algahtani et al. [39], TQ was dissolved in BSO, and then the oil was emulsified with the aqueous phase using an ultrasonication process to produce nanoemulsions that were later used to formulate nono-emulgel for wound healing applications. The loading efficiency of TQ was  $\approx 99$  %. That finding is in agreement with the current study, as the emulsification process did not have a significant impact on the stability of TQ in the BSO-ALG emulsions. Abedi et al. [40] encapsulated BSO with a mixture of modified starch-maltodextrin following a spray-drying technique. The retention of TQ in various formulations varied from 54.73 % to 61.12 % following the variation in the wall material ratios. Compared with the current study, it is difficult to detect the effect of emulsification on the stability of TQ, as the results presented were about the final formulations. Mostly, the major impact belonged to the drying action, which meets the current study about the evaporation of TQ. In their study, the highest retention of TQ was obtained at the highest solid content in the formulations; the concentration of maltodextrin was increased, which enhanced the retention of TQ against volatility. However, increasing the solid content in the current study was not applicable due to the difficulties in the beads' formation; a high viscosity would be obtained by increasing the concentration of ALG. Further studies could be conducted in order to investigate the impact of increasing the solid content on the retention of TQ in the dried formulation of BABs.

### 3.4. Stability results

#### 3.4.1. The organoleptic characteristics

The organoleptic properties of both wet and dried beads were visually investigated during the stability period of 90 days under real-

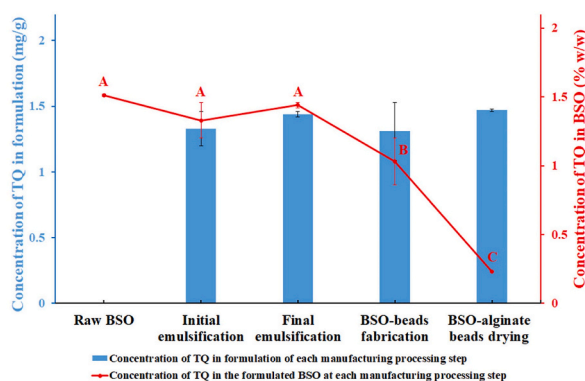


**Fig. 5.** Concentration of TQ in each processing step and in the formulated BSO at each manufacturing step. Different letters indicate significant differences among means ( $p < 0.05$ ). Error bars represent the SD of the mean values ( $n = 3$ ).

time and accelerated conditions, as shown in Fig. 6. The wet BABs appeared as milky and rubber-like beads, while the dried BABs appeared as yellowish-golden transparent beads. No changes were observed in the physical appearance and color of both wet and dried forms during storage (Fig. 6). Moreover, the formulations of BABs were stable against oil leakage and water squeezing in both wet and dried forms for 90 days of storage under real-time and accelerated conditions (Fig. 6). The stability of organoleptic characteristics might refer to the ALG type selected in the current study, which is an ALG with high stiffness gelation type. Additionally, the stability of emulsions also has a significant impact on the stability of the beads; the oil droplets would be homogeneously distributed among the beads, and then higher oil entrapment would be obtained [35].

#### 3.4.2. Changes in the size and sphericity of the manufactured beads

The average size of the wet BABs under real-time and accelerated conditions followed the same behavior during the stability study. The size was stable for the first 30 days with no significant changes ( $p > 0.05$ ), which was firstly 1.94 mm then 1.97 mm, for the real-time conditions and 1.95 mm for the accelerated conditions, as shown in Fig. 7. Later, the size slightly decreased for the second month

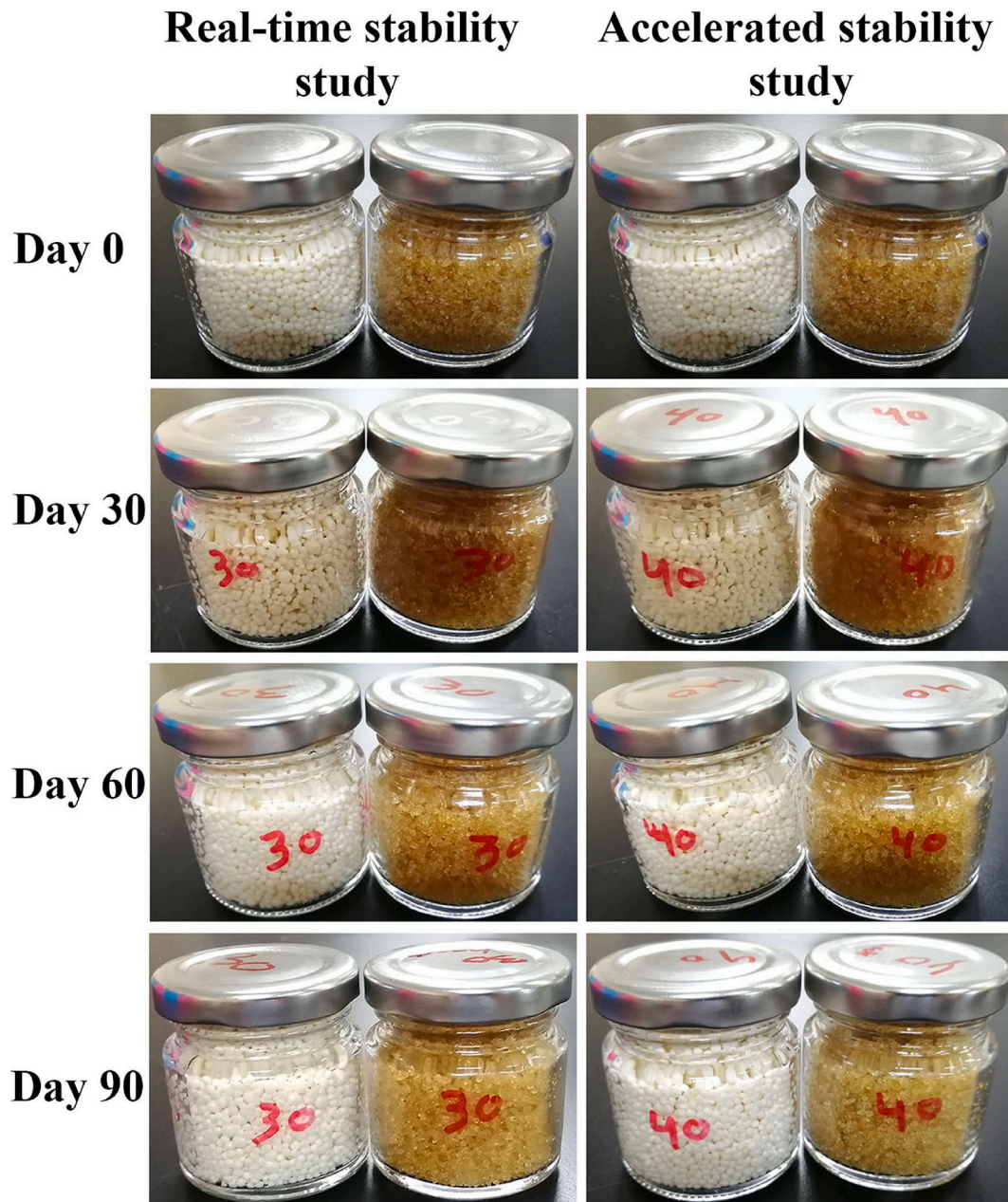


Fig. 6. Changes in the organoleptic characteristics of wet and dried BSO-ALG beads for 90 days under the real-time and accelerated conditions.

to be stable again between day 60 and day 90 with no significant difference ( $p > 0.05$ ); it ranged between 1.7 mm and 1.74 mm and between 1.71 mm and 1.73 mm for the real-time and accelerated conditions, respectively (Fig. 7A). Although the reduction in the bead size was small, a significant change ( $p < 0.05$ ) was detected statistically.

The % RSD values under both stability conditions were also calculated and found to be in agreement with the changes in bead size; an increase in %RSD values was detected after the first 30 days to be later stable, as shown in Fig. 7A. The size variation slightly increased due to the compression during storage, as the wet beads have a semisolid texture. However, the size variation was still in the acceptable range and the wet beads were able to keep their spherical shape during the storage time with SF values  $< 0.05$  on average (Figs. 7A–B).

On the other hand, BABs were more stable in the dried form than the wet form, as the rubber texture changed during the drying process and the beads became more solid. No significant changes in the dried bead size ( $p > 0.05$ ) were found during the storage for 90 days under both real-time and accelerated conditions (Figs. 7 and 8). The drying process affects the size distribution and shape of ALG beads due to the shrinking action after water loss [41], which was about 80 % of the beads in the current study. The dried beads' size was  $1.22 \pm 0.12$  mm at the beginning of the stability study, and then the size was  $1.2 \pm 0.07$  mm and  $1.11 \pm 0.11$  mm after 90 days of real-time and accelerated storage, respectively. In addition to the reduction in the beads size after drying, the SF values were  $>$  the SF values of wet beads, indicating less sphericity in the dried beads (Figs. 7 and 8). The non-spherical shapes resulted in different values of %RSD with no regular relationship, but they were generally  $>$  the %RSD values of wet bead size (Fig. 7).

### 3.4.3. Loss on drying in beads

The stability of BABs in both wet and dried forms was investigated in terms of LOD during the 90 days of storage, as shown in Fig. 9A. The initial LOD values of the wet and dried beads were 79.67 and 5.39 %, respectively. The BABs were stable during the 90 days of storage (Fig. 9A). During the storage under real-time conditions, no significant changes in LOD values were detected at day 90 ( $p > 0.05$ ), where it was 80.94 and 4.59 % for the wet and dried beads, respectively. Moreover, the accelerated conditions did not affect the stability of BABs in terms of LOD, as it was 80.34 and 4.39 % with no significant differences ( $p > 0.05$ ) compared with the initial recorded values at day 0 for both wet and dried beads, respectively (Fig. 9A). LOD stability is in good agreement with the organoleptic characteristics of BABs; the stable rate of LOD during the 90 days indicates that there was no water or oil leaking out of the beads, which represents a good appearance for the formulations.

### 3.4.4. Stability of TQ

The stability of TQ in BABs in both wet and dried forms was not in real agreement with the physical stability of the beads, as shown

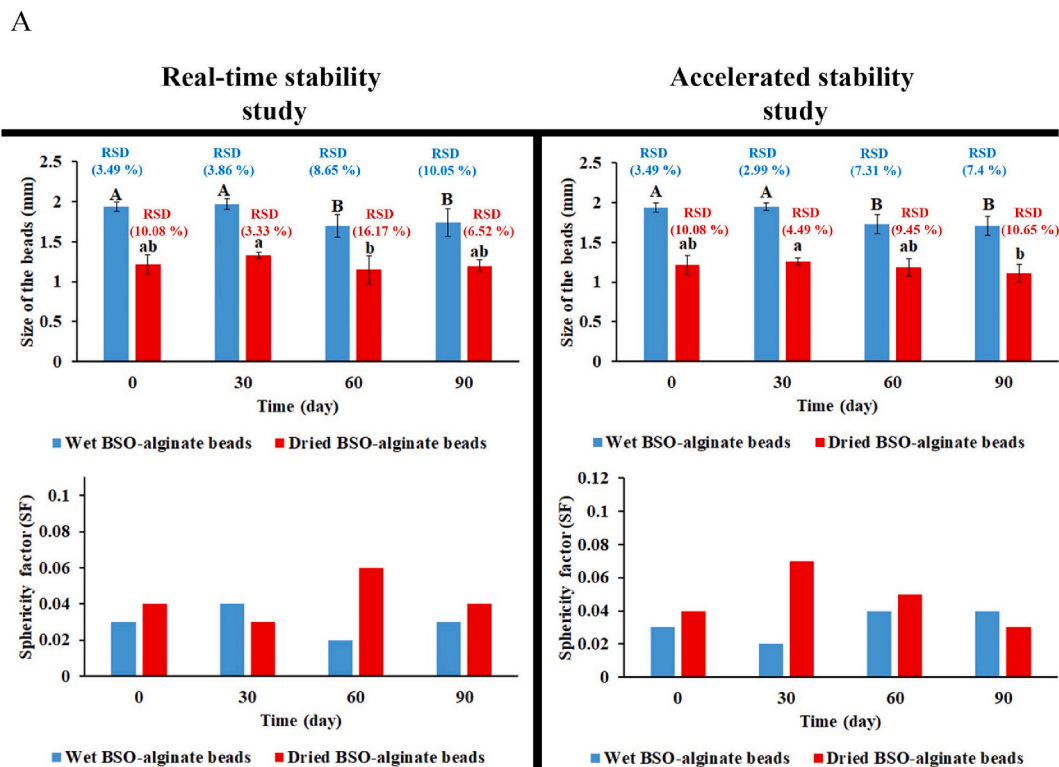


**Fig. 7A.** Changes in the size and sphericity of wet and dried BSO-ALG beads for 90 days under the real-time and accelerated conditions. Different letters indicate significant differences among means ( $p < 0.05$ ). Error bars represent the standard deviation of the mean values ( $n = 10-15$ ).

B

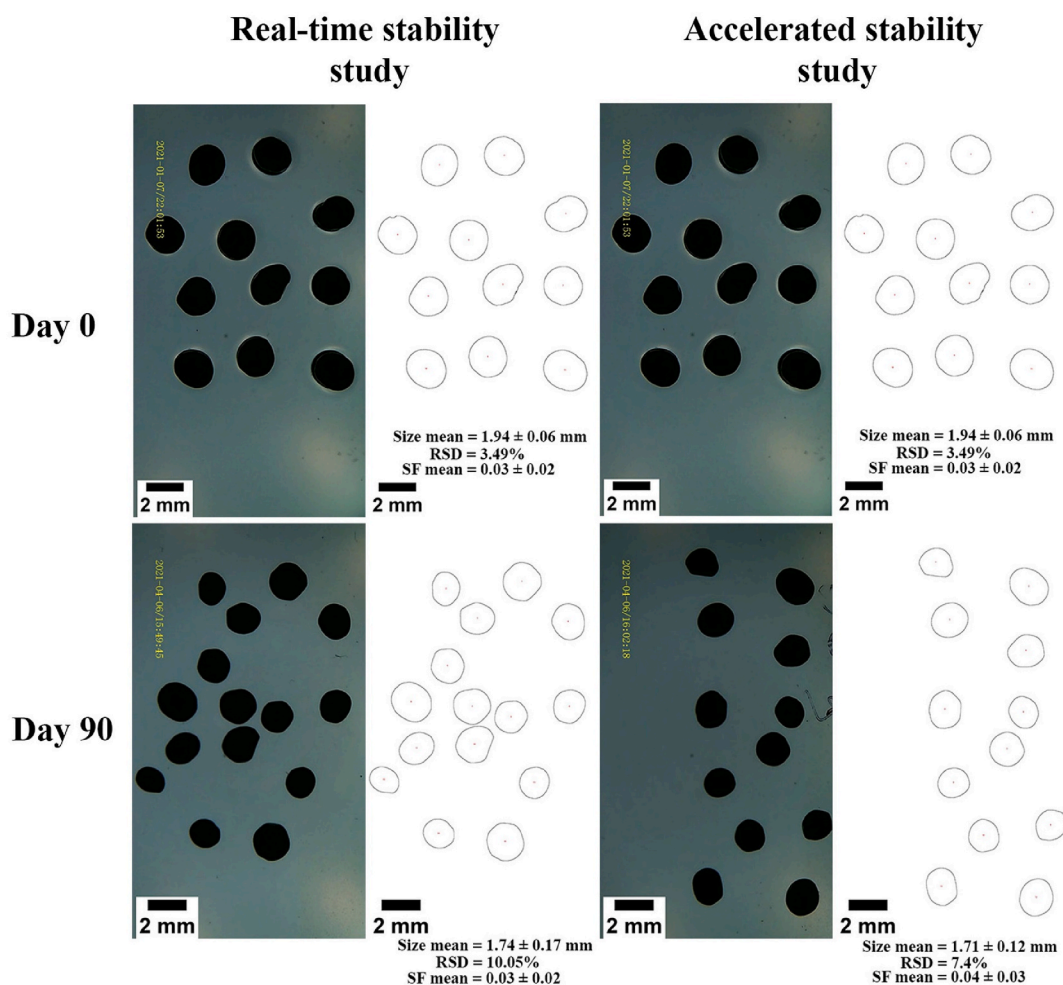


**Fig. 7B.** Image of the wet BSO-ALG beads and processed image for measurement analysis using Image J software under real-time and accelerated stability conditions for 90 days.

in the stability of organoleptic characteristics, size and sphericity, and LOD. However, changes in TQ in the wet BABs behaved similarly in both real-time and accelerated conditions (Fig. 9B–C). The initial concentration of TQ at day 0 in the wet beads was  $1.5 \pm 0.27$  mg/g, then changed to 1.44 and 1.57 mg/g at day 30 in both real-time and accelerated conditions, respectively, with no significant difference in both conditions ( $p > 0.05$ ), as shown in Fig. 9B. Moreover, the stability of TQ was affected significantly at day 60 ( $p < 0.05$ ); then its content was stable at 0.83 mg/g (44.26 % < the initial concentration) and 0.69 mg/g (53.4 % < the initial concentration) for the real-time and accelerated conditions, respectively. There was no significant difference for both conditions ( $p > 0.05$ ), as depicted in Fig. 9B.

Fig. 9B–C shows the changes in TQ in dried BABs; TQ content reduced significantly from 1.47 mg/g at day 0–0.61 mg/g (58.7 % < the initial concentration) and 0.23 mg/g (83.8 % < the initial concentration) after 90 days of storage ( $p < 0.05$ ) for the real-time and accelerated conditions, respectively. Based on the obtained results, encapsulation of BSO on ALG beads in the wet form had the ability to stabilize TQ > the dried form, which was clearer in the accelerated stability data.

The stability of TQ was studied before in different environments and it was found to be unstable in oxidative conditions [9]. However, the oxidation of edible oils could be affected by some factors, such as heat, light, or the presence of metals, that could accelerate or cause oxidation [42]. The accelerated conditions provide a higher temperature that could accelerate any possible oxidation. Moreover, the appearance of the dried beads was found to be transparent, while the wet beads were found cloudy or milky. The dim appearance of wet beads might be one of the reasons for lower oxidation, resulting in greater stability of TQ. Alamed et al. [43] studied the effect of calcium ions on the oxidation of salmon oil in oil-in-water emulsions. The calcium ions were provided as a  $\text{CaCl}_2$  solution added to the emulsion. It was found that exceeding a certain level of calcium significantly increased hydroperoxide formation. One of the most common factors that causes oil oxidation is the interaction between the hydroperoxides that are present on the droplet

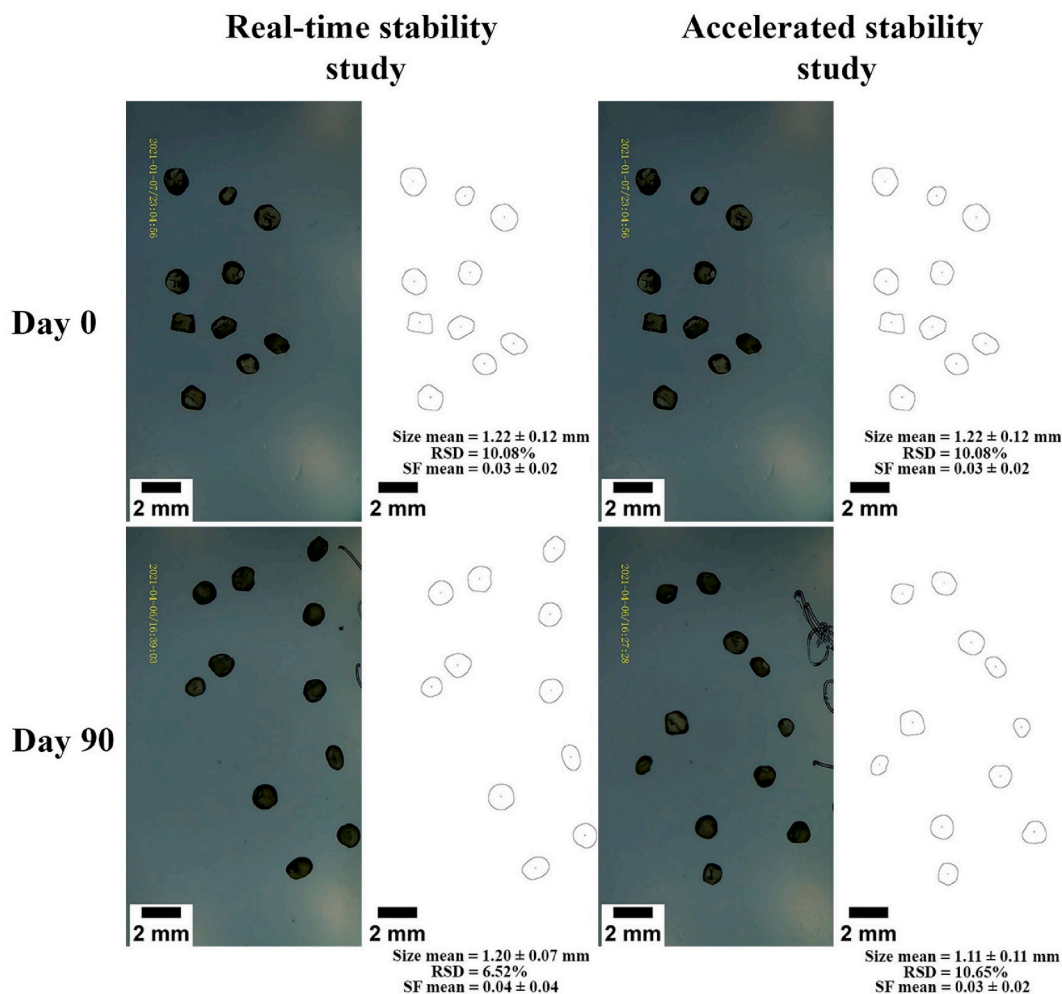
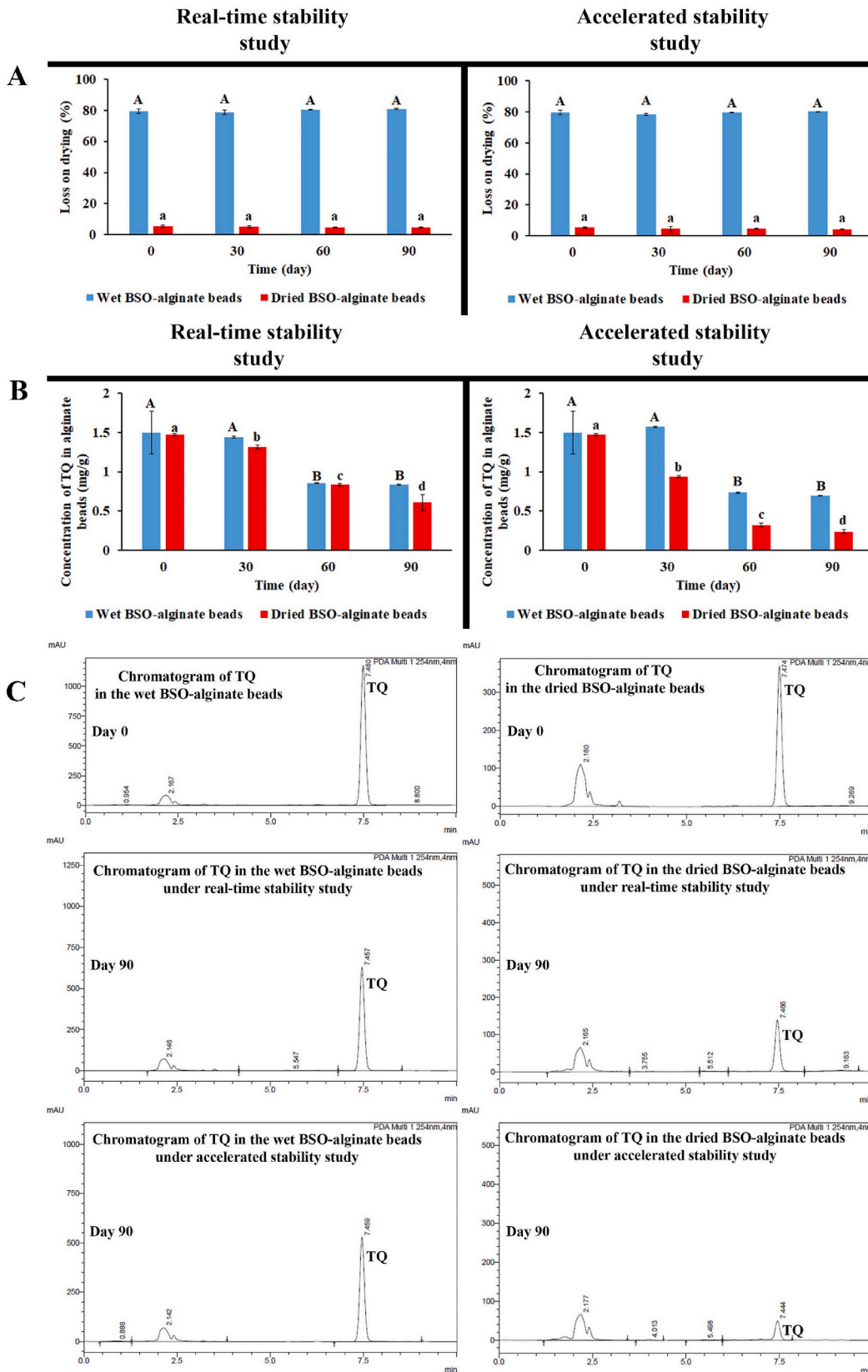


**Fig. 8.** Image of the dried BSO-ALG beads and processed image for measurement analysis using Image J software under real-time and accelerated stability conditions for 90 days.

surface and metals in the aqueous phase.

In this regard, calcium ions might also be another possible reason behind TQ degradation in the beads, in agreement with the obtained results. Firstly, the oil quantity in each single bead is the same in both wet and dried beads, but the concentration of calcium ions in each form is different; 80 % of the wet bead is water. Thus, calcium ions in the dried bead are more concentrated than in the wet bead. On the other hand, BSO in the dried bead is closer to the surrounding air than in the wet bead, where the BSO in the wet bead is still considered to be distributed droplets in the continuous aqueous phase, making a complete surface of droplets, followed by the surrounding aqueous phase. Therefore, TQ was found to be more stable in the wet BABs. In the study of Tubesha et al. [44], TQ was formulated in an oil-in-water nanoemulsion by emulsifying Triolein that contains TQ with the aqueous phase composed of Tween-80 and double-distilled water. The stability of TQ was evaluated for 6 months under 4, 25, and 40 °C. The retention of TQ in the samples for all conditions was approximately 90 % (about a 10 % difference compared with the initial concentration in the formulation). By comparing this finding with the data of Salmani et al. [9], it is observable that TQ tends to be more stable in the oil phase > pure TQ in aqueous formulations. It is also notable that no source of metals was used to formulate the TQ nanoemulsions compared with the current study; we used  $\text{CaCl}_2$  in the gelation bath, which would be a reason behind the stability of TQ in the nanoemulsion formulation.

In light of food preservation and food safety, the current finding highlights the effectiveness of microencapsulation through the ionic gelation of alginate in stabilizing and delivering TQ, particularly when formed as wet hydrogel beads. The drying process, commonly used to remove water content, can significantly impact the stability of TQ, a volatile compound. Therefore, the utilization of wet alginate emerges as a notable strategy for reformulating volatile compounds commonly found in their original products, which often encounter delivery challenges. These findings are robust, as they were obtained from samples stored under a stability study conducted at a pilot scale production level. This aspect confirms the reproducibility, validates the feasibility, and the capability of the production methods utilized.



(caption on next page)

**Fig. 9.** Loss on drying (A) and stability of TQ (B) in wet and dried BSO-ALG beads for 90 days under the real-time and accelerated conditions. Different letters indicate significant differences among means ( $p < 0.05$ ). Error bars represent the standard deviation of the mean values ( $n = 3$ ), and HPLC chromatogram (C) of TQ in wet/dried BSO-ALG beads for 90 days in real-time and accelerated conditions.

#### 4. Conclusion

The ionic gelation-based formulation of BABs was successfully scaled up to the pilot scale of 50 kg batch size. Firstly, the BSO-ALG emulsion was obtained by applying two emulsification steps, namely the initial and final emulsification processes. Thereafter, 12 units of 3D-printed multi-nozzles (22-gauge) were employed to drip the final emulsion into the gelation/curing bath of  $\text{CaCl}_2$  at a dripping flow rate of 288 mL/min. The formed beads were washed and filtered using a 50 L vacuum suction filtration system. The drying process was applied to provide another option as a finished product. The BABs were manufactured with consistent quality. In the current study, the effect of the manufacturing process on the TQ stability was also evaluated. A dramatic drop in the concentration of TQ within BSO was found after drying the beads. Additionally, the wet pilot scale manufactured BABs were physically stable and their ability to stabilize TQ was higher than that of the dried beads, making them a good candidate to naturally supply TQ. However, more investigations on TQ have to be carried out in the future in order to enhance TQ stability. The outcomes of this study not only enable large-scale manufacturing of encapsulated BSO and similar bioactive compounds but also emphasize the comprehensive implications for microencapsulation technology. These advancements hold promise for enhancing food preservation, safety, and therapeutic delivery methods.

#### Data availability

The data are available upon reasonable request.

#### CRediT authorship contribution statement

**Hamzeh Alkhatib:** Writing – review & editing, Writing – original draft, Visualization, Validation, Software, Methodology, Investigation, Formal analysis, Data curation, Conceptualization. **Farahidah Mohamed:** Writing – review & editing, Supervision, Resources. **Mulham Alfatama:** Writing – review & editing, Methodology, Data curation. **Elham Assadpour:** Writing – review & editing, Investigation, Formal analysis. **Mohammad Saeed Kharazmi:** Writing – review & editing, Investigation, Formal analysis. **Seid Mahdi Jafari:** Writing – review & editing, Visualization, Validation, Resources, Investigation, Formal analysis, Data curation. **Md Zaidul Islam Sarker:** Methodology, Formal analysis, Data curation. **Kishor Kumar Sadasivuni:** Writing – review & editing, Validation, Funding acquisition. **Awis Sukarni Mohmad Sabere:** Writing – review & editing, Supervision, Project administration, Funding acquisition. **Abd Almonem Doolaanea:** Writing – review & editing, Visualization, Supervision, Resources, Project administration, Funding acquisition, Conceptualization.

#### Declaration of competing interest

The authors declare the following financial interests/personal relationships which may be considered as potential competing interests:

Abd Almonem Doolaanea and Awis Sukarni Mohmad Sabere reports financial support was provided by Malaysian Ministry of Science, Technology, and Innovation (MOSTI). If there are other authors, they declare that they have no known competing financial interests or personal relationships that could have appeared to influence the work reported in this paper.

#### Acknowledgements

The authors would like to thank I-KOP Sdn. Bhd (GMP licensed pharmaceutical manufacturer) for technical and facilitation support. This study was supported by the Malaysian Ministry of Science, Technology, and Innovation (MOSTI) grant number SR1017Q1038/SMF18-001-0001.

#### Appendix A. Supplementary data

Supplementary data to this article can be found online at <https://doi.org/10.1016/j.heliyon.2024.e37630>.

#### References

- [1] Y. Mazaheri, et al., A comprehensive review of the physicochemical, quality and nutritional properties of *Nigella sativa* oil, *Food Rev. Int.* 35 (4) (2019) 342–362.
- [2] H. Mukhtar, et al., *Nigella sativa* L. seed and seed oil: potential sources of high-value components for development of functional foods and nutraceuticals/pharmaceuticals, *J. Essent. Oil Res.* 31 (3) (2019) 171–183.

- [3] H. Alkhatib, et al., Thymoquinone content in marketed black seed oil in Malaysia, *J. Pharm. BioAllied Sci.* 12 (3) (2020) 284.
- [4] M. Talebi, et al., Biological and therapeutic activities of thymoquinone: focus on the Nrf2 signaling pathway, *Phytother. Res.* 35 (4) (2021) 1739–1753.
- [5] Z.A. Hawsawi, B.A. Ali, A.O. Bamosa, Effect of *Nigella sativa* (black seed) and thymoquinone on blood glucose in albino rats, *Ann. Saudi Med.* 21 (3–4) (2001) 242–244.
- [6] B. Almajali, et al., Thymoquinone, as a novel therapeutic candidate of cancers, *Pharmaceuticals* 14 (4) (2021) 369.
- [7] M.R. Khazdair, S. Ghafari, M. Sadeghi, Possible therapeutic effects of *Nigella sativa* and its thymoquinone on COVID-19, *Pharmaceut. Biol.* 59 (1) (2021) 696–703.
- [8] H. Xu, et al., Computational and experimental studies reveal that thymoquinone blocks the entry of coronaviruses into in vitro cells, *Infectious diseases and therapy* 10 (1) (2021) 483–494.
- [9] J.M.M. Salmani, et al., Aqueous solubility and degradation kinetics of the phytochemical anticancer thymoquinone; probing the effects of solvents, pH and light, *Molecules* 19 (5) (2014) 5925–5939.
- [10] H. Alkhatib, et al., Microencapsulation of black seed oil in alginate beads for stability and taste masking, *J. Drug Deliv. Sci. Technol.* 60 (2020) 102030.
- [11] J.-Y. Leong, et al., Advances in fabricating spherical alginate hydrogels with controlled particle designs by ionotropic gelation as encapsulation systems, *Particuology* 24 (2016) 44–60.
- [12] D. Jain, D. Bar-Shalom, Alginate drug delivery systems: application in context of pharmaceutical and biomedical research, *Drug Dev. Ind. Pharm.* 40 (12) (2014) 1576–1584.
- [13] K.Y. Lee, D.J. Mooney, Alginate: properties and biomedical applications, *Prog. Polym. Sci.* 37 (1) (2012) 106–126.
- [14] C.J. Patel, et al., Pharmaceutical taste masking technologies of bitter drugs: a concise review, *J. Drug Discov. Therapeut* 1 (5) (2013) 39–46.
- [15] M. Levin, *Pharmaceutical Process Scale-Up*, second ed., CRC Press, 2006.
- [16] C. Heinzen, et al., Use of Vibration Technology for Jet Break-Up for Encapsulation of Cells, Microbes and Liquids in Monodisperse Microcapsules, SH241, Landbauforschung Völkrode, 2002, pp. 19–25.
- [17] B.B. Lee, P. Ravindra, E.S. Chan, Size and shape of calcium alginate beads produced by extrusion dripping, *Chem. Eng. Technol.* 36 (10) (2013) 1627–1642.
- [18] Y. Apsarina, C. Anam, L.U. Khasanah, The impact of blending speed and duration on the characteristics of powdered milk product X in PT. XYZ, in: AIP Conference Proceedings, AIP Publishing LLC, 2020.
- [19] İ.G. Erdem, M.M. Ak, Gelation characteristics of sodium alginate in presence of flavor molecules, *J. Food Process. Preserv.* 45 (1) (2021) e15033.
- [20] A. Belščak-Cvitanović, et al., Improving the controlled delivery formulations of caffeine in alginate hydrogel beads combined with pectin, carrageenan, chitosan and psyllium, *Food Chem.* 167 (2015) 378–386.
- [21] S. Maharjan, N. Prajapati, A. Shrestha, Formulation and evaluation of sustained release sodium alginate beads of indomethacin, *Asian Journal of Pharmacy and Technology* 2 (8.00) (2019) 100, 00.
- [22] H. Alkhatib, et al., Emulsification-assisted spectroscopic analysis of black seed oil in alginate beads: method development and validation, *Analytical Chemistry Letters* 13 (3) (2023) 234–243.
- [23] ASEAN, Association of South East Asian Nations (ASEAN) Guideline on Stability Study and Shelf-Life of Drug Product, 2013.
- [24] ICH, International Council for Harmonization (ICH), Guideline on Stability testing of new drug substances and products, Q1A (R2), current step 4 (2003) 1–24.
- [25] N. Provenza, et al., Design and physicochemical stability studies of paediatric oral formulations of sildenafil, *Int. J. Pharm.* 460 (1–2) (2014) 234–239.
- [26] T. Delompré, et al., Taste perception of nutrients found in nutritional supplements: a review, *Nutrients* 11 (9) (2019) 2050.
- [27] C. Jeong, et al., Changes in the physical properties of calcium alginate gel beads under a wide range of gelation temperature conditions, *Foods* 9 (2) (2020) 180.
- [28] M. Paris, et al., Modelling release mechanisms of cinnamon (*Cinnamomum zeylanicum*) essential oil encapsulated in alginate beads during vapor-phase application, *J. Food Eng.* 282 (2020) 110024.
- [29] L. Agüero, et al., Alginate microparticles as oral colon drug delivery device: a review, *Carbohydr. Polym.* 168 (2017) 32–43.
- [30] F.L. Lopez, et al., Formulation approaches to pediatric oral drug delivery: benefits and limitations of current platforms, *Expet Opin. Drug Deliv.* 12 (11) (2015) 1727–1740.
- [31] N.T.T. Uyen, et al., Fabrication of alginate microspheres for drug delivery: a review, *Int. J. Biol. Macromol.* 153 (2020) 1035–1046.
- [32] D. Lin, et al., Effect of structuring emulsion gels by whey or soy protein isolate on the structure, mechanical properties, and in-vitro digestion of alginate-based emulsion gel beads, *Food Hydrocolloids* 110 (2021) 106165.
- [33] M. Maleki, et al., Study on liquid core barberry (*Berberis vulgaris*) hydrogel beads based on calcium alginate: effect of storage on physical and chemical characterizations, *J. Food Process. Preserv.* 44 (5) (2020) e14426.
- [34] L. Cao, et al., Egg-box model-based gelation of alginate and pectin: a review, *Carbohydr. Polym.* 242 (2020) 116389.
- [35] J.A. Piornos, et al., Highly efficient encapsulation of linseed oil into alginate/lupin protein beads: optimization of the emulsion formulation, *Food Hydrocolloids* 63 (2017) 139–148.
- [36] K.F.C. e Silva, et al., Sacha inchi oil encapsulation: emulsion and alginate beads characterization, *Food Bioprod. Process.* 116 (2019) 118–129.
- [37] I. Rahat, et al., Thymoquinone-entrapped chitosan-modified nanoparticles: formulation optimization to preclinical bioavailability assessments, *Drug Deliv.* 28 (1) (2021) 973–984.
- [38] I. Baldim, et al., Factors affecting the retention efficiency and physicochemical properties of spray dried lipid nanoparticles loaded with *lippia sidoides* essential oil, *Biomolecules* 10 (5) (2020) 693.
- [39] M.S. Algahtani, et al., Thymoquinone loaded topical nanoemulgel for wound healing: formulation design and in-vivo evaluation, *Molecules* 26 (13) (2021) 3863.
- [40] A.S. Abedi, et al., A mixture of modified starch and maltodextrin for spray drying encapsulation of *Nigella sativa* seeds oil containing thymoquinone, *Starch Staerke* 73 (3–4) (2021) 1900255.
- [41] E.-S. Chan, Preparation of Ca-alginate beads containing high oil content: influence of process variables on encapsulation efficiency and bead properties, *Carbohydr. Polym.* 84 (4) (2011) 1267–1275.
- [42] E. Choe, D.B. Min, Mechanisms and factors for edible oil oxidation, *Compr. Rev. Food Sci. Food Saf.* 5 (4) (2006) 169–186.
- [43] J. Alamed, D.J. McClements, E.A. Decker, Influence of heat processing and calcium ions on the ability of EDTA to inhibit lipid oxidation in oil-in-water emulsions containing omega-3 fatty acids, *Food Chem.* 95 (4) (2006) 585–590.
- [44] Z. Tubesha, Z. Abu Bakar, M. Ismail, Characterization and stability evaluation of thymoquinone nanoemulsions prepared by high-pressure homogenization, *J. Nanomater.* 2013 (2013).